Anal. Chem. **2002,** *74,* 336−346

Ion Parking during Ion/Ion Reactions in Electrodynamic Ion Traps

Scott A. McLuckey,* Gavin E. Reid, and J. Mitchell Wells

Department of Chemistry, Purdue University, West Lafayette, Indiana 47907-1393

Under appropriate ion density conditions, it is possible to selectively inhibit rates of ion/ion reactions in a quadrupole ion trap via the application of oscillatory voltages to one or more electrodes of the ion trap. The phenomenon is demonstrated using dipolar resonance excitation applied to the end-cap electrodes of a three-dimensional quadrupole ion trap. The application of a resonance excitation voltage tuned to inhibit the ion/ion reaction rate of a specific range of ion mass-to-charge ratios is referred to as "ion parking". The bases for rate inhibition are (i) an increase in the relative velocity of the ion/ion reaction pair, which reduces the cross section for ion/ion capture and, at least in some cases, (ii) reduction in the time of physical overlap of positively charged and negatively charged ion clouds. The efficiency and specificity of the ion parking experiment is highly dependent upon ion densities, trapping conditions, ion charge states, and resonance excitation conditions. The ion parking experiment is illustrated herein along with applications to the concentration of ions originally present over a range of charge states into a selected charge state and in the selection of a particular ion from a set of ions derived from a simple protein mixture.

Ionization methods have been introduced within the past fifteen years that can produce multiply charged ions from large polyatomic molecules. These methods include electrospray ionization (ESI),[1−3] massive cluster impact ionization,[4] and matrix-assisted laser desorption/ionization (MALDI).[5] Electrospray and MALDI in particular have become the ionization methods of choice for most large polyatomic molecules including peptides, proteins, oligonucleotides, carbohydrates, and synthetic polymers. In the case of MALDI, singly charged ions usually dominate.[6] However, in the case of ESI, a distribution of charge states, all of which are substantially greater than +1 or −1, usually dominate the mass spectrum of a macromolecule. While the multiple-charging phenomenon associated with ESI is an attractive feature for many analysis scenarios, it is often desirable to be able to alter the initial charge-state distribution. Examples of such cases include the manipulation of parent ion charges for the purpose of facilitating mixture analysis,[7−9] for forming (lower) ion charge states than those formed directly via ESI[10−14] for subsequent study, and for manipulating product ion charge states for the purpose of determining product ion charge.[15−18]

A number of techniques have been introduced to manipulate ion charge associated with high-mass multiply charged ions. These have included manipulation of solution conditions,[19] in the case of ESI, or matrix conditions,[6] in the case of MALDI, and the use of ion chemistry to reduce ion charge in the gas phase. Numerous examples have been shown in which ion/molecule proton-transfer reactions have been used to manipulate ion charge.[10−12,15,16,20−26] In the case of multiply protonated molecules, strong neutral bases have been admitted into a region in which ion/molecule proton-transfer reactions can occur. This has been done, for example, in ESI interfaces,[10,24] in quadrupole ion traps,[12,15,20] in the collision cells of triple quadrupole instruments,[16,22] and in Fourier transform ion cyclotron resonance (FTICR) mass spectrometers.[21,25,26] An

* Corresponding author: (phone) (765)494-5270; (fax) (765)494-0239; (e-mail) mcluckey@purdue.edu.

(1) Fenn, J. B.; Mann, M.; Meng, C. K.; Wong, S. F.; Whitehouse, C. M. *Science* **1989**, *246*, 64−71.
(2) Gaskell, S. J. *J. Mass Spectrom.* **1997**, *37*, 677−688.
(3) Cole. R. B., Ed. *Electrospray Ionization Mass Spectrometry*; Wiley-Interscience: New York, 1997.
(4) Mahoney, J. F.; Perel, J.; Ruatta, S. A.; Martino, P. A.; Husain, S.; Lee, T. D. *Rapid Commun. Mass Spectrom.* **1991**, *5*, 441−445.
(5) Karas, M.; Hillenkamp, F. *Anal. Chem.* **1988**, *60*, 2301−2303.
(6) Karas, M.; Glückmann, M.; Schäfer, J. *J. Mass Spectrom.* **2000**, *35*, 1−12.
(7) Stephenson, J. L., Jr.; McLuckey, S. A. *Anal. Chem.* **1996**, *68*, 4026−4032.
(8) Stephenson, J. L., Jr.; McLuckey, S. A. *J. Am. Soc. Mass Spectrom.* **1998**, *9*, 585−596.
(9) Stephenson, J. L., Jr.; McLuckey, S. A. *J. Mass Spectrom.* **1998**, *33*, 664−672.
(10) Clemmer, D. E.; Jarrold, M. F. *J. Mass Spectrom.* **1997**, *32*, 577−592.
(11) Smith, R. D.; Cheng, X.; Bruce, J. E.; Hofstadler, S. A.; Anderson, G. A. *Nature* **1994**, *369*, 137−139.
(12) McLuckey, S. A.; Goeringer, D. E. *Anal. Chem.* **1995**, *67*, 2493−2497.
(13) Wells, J. M.; Stephenson, J. L., Jr.; McLuckey, S. A. *Int. J. Mass Spectrom.* **2000**, *203*, A1−A9.
(14) Reid, G. E.; Wu, J.; Chrisman, P. A.; Wells, J. M.; McLuckey, S. A. *Anal. Chem.* **2001**, *73*, 3274−3281.
(15) McLuckey, S. A.; Glish, G. L.; Van Berkel, G. J. *Anal. Chem.* **1991**, *63*, 1971−1978.
(16) Hunter, A. P.; Severs, J. C.; Harris, F. M.; Games, D. E. *Rapid Commun. Mass Spectrom.* **1994**, *8*, 417−422.
(17) Herron, W. J.; Goeringer, D. E.; McLuckey, S. A. *Anal. Chem.* **1996**, *10*, 277−281.
(18) Stephenson, J. L., Jr.; McLuckey, S. A. *Anal. Chem.* **1998**, *70*, 3533−3544.
(19) Muddiman, D. C.; Cheng, X.; Udseth, H. R.; Smith, R. D. *J. Am. Soc. Mass Spectrom.* **1996**, *7*, 697−706.
(20) McLuckey, S. A.; Van Berkel, G. J.; Glish, G. L. *J. Am. Chem. Soc.* **1990**, *112*, 5668−5670.
(21) Williams, E. R. *J. Mass Spectrom.* **1996**, *31*, 831−842.
(22) Loo, R. R. O.; Loo, J. A.; Udseth, H. R.; Fulton, J. L.; Smith, R. D. *Rapid Commun. Mass Spectrom.* **1992**, *6*, 159−165.
(23) Winger, B. E.; Light-Wahl, K. J.; Smith, R. D. *J. Am. Soc. Mass Spectrom.* **1992**, *3*, 624−630.
(24) Ikonomou, M. G.; Kebarle, P. *Int. J. Mass Spectrom. Ion Processes* **1992**, *117*, 283−298.
(25) Gross, D. S.; Williams, E. R. *J. Am. Chem. Soc.* **1995**, *117*, 883−890.
(26) Cassady, C. J.; Carr, S. R. *J. Mass Spectrom.* **1996**, *31*, 247−254.

10.1021/ac0109671 CCC: $22.00
Published on Web 12/08/2001

advantage to the use of ion/molecule reactions for charge-state manipulation is that the reactions are readily effected in many types of instruments in that they simply require the admission of a gaseous reactant within a suitable reaction region. However, the extent to which charge states can be reduced in multiply charged ions is limited[27] and is dependent upon many factors including the acidity or basicity of the neutral molecule and structural characteristics of the macroion. Furthermore, clustering reactions can compete with charge transfer. An additional complexity for ion trapping instruments is associated with the fact that most neutral reagents that undergo proton-transfer chemistry are relatively polar such that it is difficult to admit and remove the reagents rapidly enough to avoid charge permutation reactions at inconvenient times in the experiment.

The use of ions of charge opposite to the macroions of interest overcomes the limitations associated with the use of neutral reagents to effect charge-state manipulation. For example, all ion/ion reactions are highly exothermic such that charge states can be reduced to arbitrarily low values, including zero.[28] By use of the appropriate ions, clustering reactions can be avoided. For example, it has been demonstrated that anions derived from glow discharge ionization of perfluorocarbons react exclusively by proton transfer with multiply protonated proteins.[28,29] Finally, the introduction and removal of ions from a reaction region can be controlled much more readily than the introduction and removal of neutral molecules. Ion/ion reactions have been conducted both prior to introduction of ions into a mass spectrometer[30−33] and after ions have been accumulated in ion trapping instruments.[7−9,13,14,18,28,29,34−38] The former approach enjoys the advantage of simplicity in that it can be effected with virtually any form of ion analyzer. The latter approach enjoys the advantages of MS/MS whereby ions of either or both polarities can be manipulated in various ways and for various purposes. For example, it is straightforward to subject product ions derived from the dissociation of a mass-selected multiply charged parent ion to proton-transfer reactions with ions of opposite charge in an ion trapping instrument whereas such an experiment is not possible when ion/ion reactions are effected outside of the mass spectrometer. In fact, by use of MS^n strategies, it has been demonstrated that two stages of ion/ion reactions can be used in a single experiment.[14,39] For example, the first stage of the experiment can be used to form parent ion charge states that are not formed directly by ESI. The second ion/ion reaction period can be applied to product ions formed from the dissociation of a low-charge-state parent ion formed in the preceding ion/ion reaction period. By far, most work has been conducted with quadrupole ion traps in which ions of opposite polarity can be stored simultaneously and in overlapping regions of space.

A particularly important characteristic of ion trapping instruments, such as electrodynamic ions traps[40] and ion cyclotron resonance traps,[41] is that ions execute mass-to-charge-dependent frequencies of motion. This characteristic can be exploited to affect the rates of ion/ion reactions of ions in a quadrupole ion trap in a mass-to-charge selective fashion. The inhibition of ion/ion reactions for *selected* ions is denoted herein as "ion parking". Ion parking enables several analytically useful capabilities for the analysis of mixtures and for the study of the chemistry of high-mass multiply charged ions. In this report, we describe the basis for ion parking and illustrate its utility for the selective accumulation of particular charge state macroions in the case of a single analyte molecule and in the case of multiply charged ions derived from a simple protein mixture.

EXPERIMENTAL SECTION

Bovine cytochrome *c* and horse heart myoglobin were obtained from Sigma (St. Louis, MO). Perfluoro-1,3 dimethylcyclohexane (PDCH) was purchased from Aldrich (Milwaukee, WI). Solutions for electrospray were prepared by dissolving quantities of either myoglobin or cytochrome *c* or both to result in concentrations of ~5 μM/protein in methanol/water/acetic acid (50:49:1). Electrospray solutions were delivered to a stainless steel electrospray capillary via a syringe pump with a flow rate of 1 μL/min. Typically, the voltage applied to the capillary needle ranged from +3.0−3.5 kV.

All experiments were performed with a homemade electrospray source coupled to a Finnigan-MAT (San Jose, CA) ion trap mass spectrometer[42] that has been modified for the addition of negatively charged (PDCH) ions through a hole in the ring electrode.[29] A typical scan function used in this study featured positive ion accumulation (20−100 ms), anion injection (1−3 ms), mutual cation/anion storage (100−300 ms), and mass analysis using resonance ejection.

The spectra recorded after ion/ion reactions were used to reduce ion charge states are referred to as post-ion/ion mass spectra. Resonance ejection for these post-ion/ion spectra was performed at either 17 000 Hz, and 1.5 V_{p-p} to give an upper mass-to-charge limit of 13 000 or 89 202 Hz and 9.8 V_{p-p} to give an upper mass-to-charge limit of 2400. Each mass spectrum presented herein is the average of 100−300 scans.

RESULTS AND DISCUSSION

The essential concept behind ion parking during ion/ion reactions in an ion trap is to inhibit the rate of ion/ion proton-transfer reactions in a selective fashion such that particular ions

(27) McLuckey, S. A.; Van Berkel, G. J.; Glish, G. L.; Schwartz, J. C. In *Practical Aspects of Ion Trap Mass Spectrometry. Vol. II: Ion Trap Instrumentation*; March, R. E., Todd, J. F. J., Eds.; CRC Press: Boca Raton, FL, 1995; Chapter 3, pp 89−141.

(28) Stephenson, J. L., Jr.; McLuckey, S. A. *J. Am. Chem. Soc.* **1996**, *118*, 7390−7397.

(29) Stephenson, J. L., Jr.; McLuckey, S. A. *Int. J. Mass Spectrom. Ion Processes* 1997, *162*, 89−106.

(30) Loo, R. R. O.; Udseth, H. R.; Smith, R. D. *J. Phys. Chem.* **1991**, *95*, 6412−6415.

(31) Loo, R. R. O.; Udseth, H. R.; Smith R. D. *J. Am. Soc. Mass Spectrom.* **1992**, *3*, 395−405.

(32) Scalf, M.; Westphall, M. S.; Krause, J.; Kaufman, S. L.; Smith, L. M. *Science* **1999**, *283*, 194−197.

(33) Scalf, M.; Westphall, M. S.; Smith, L. M. *Anal. Chem.* **2000**, *72*, 52−60.

(34) Herron, W. J.; Goeringer, D. E.; McLuckey, S. A. *J. Am. Soc. Mass Spectrom.* **1995**, *6*, 529−532.

(35) Herron, W. J.; Goeringer, D. E.; McLuckey, S. A. *J. Am. Chem. Soc.* **1995**, 117, 11555−11562.

(36) McLuckey, S. A.; Stephenson, J. L., Jr. *Mass Spectrom. Rev.* **1998**, *17*, 369−407.

(37) Payne, A. H.; Glish, G. L. *Int. J. Mass Spectrom.* **2001**, *204*, 47−54.

(38) McLuckey, S. A.; Wells, J. M.; Stephenson, J. L., Jr.; Goeringer, D. E. *Int. J. Mass Spectrom.* **2000**, *200*, 137−161.

(39) Stephenson, J. L., Jr.; McLuckey, S. A. *J. Am. Chem. Soc.* **1997**, *119*, 1688−1696.

(40) March, R. E. *J. Mass Spectrom.* **1997**, *32*, 351−369.

(41) Marshall, A. G.; Hendrickson, C. L.; Jackson, G. S. *Mass Spectrom. Rev.* **1998**, *17*, 1−35.

(42) McLuckey, S. A.; Stephenson, J. L., Jr.; Asano, K. G. *Anal. Chem.* **1998**, *70*, 1198−1202.

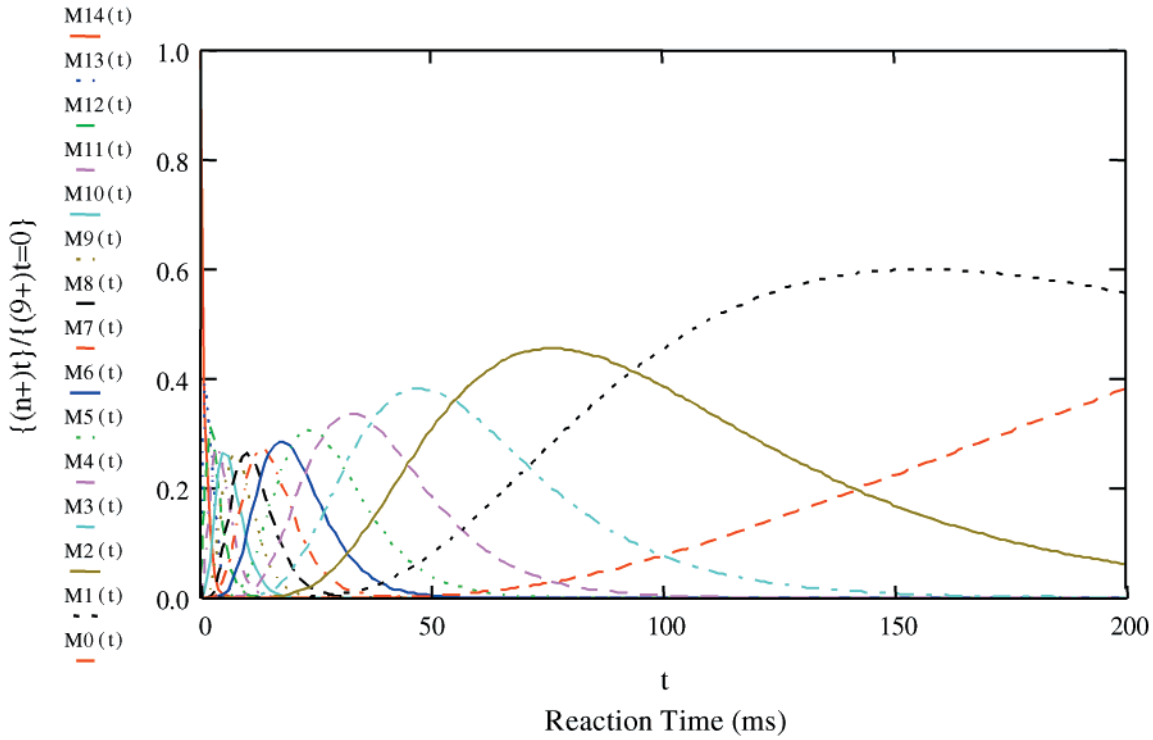

Figure 1. Predicted time evolution of the positive ion abundances resulting from the reaction of the +14 charge state of cytochrome *c* with an excess of singly charged negative ions. The plot reflects a series of consecutive irreversible reactions in which the +1/−1 reaction rate is 5 s^{-1} and all other reaction rates scale as the square of the charges of the ionic reactants.

tend to be preferentially retained in the ion trap, while ions that are not selected undergo neutralization reactions unperturbed. Several important characteristics of ion/ion reactions and ion motion in an ion trap play important roles in determining how to effect ion parking and the mass-to-charge specificity with which ion/ion reactions can be inhibited. These essential characteristics are described below with particular emphasis on their relationships to ion parking.

Ion/Ion Reaction Kinetics. All ion/ion reactions studied to date in quadrupole ion traps have taken place in the presence of a light bath gas, predominantly helium, at a pressure of roughly 1 mTorr. It has been noted that ion/ion proton-transfer kinetics operated under these conditions are related to the square of the charges of the reactant ions.[28,42] The magnitudes of the observed ion/ion reaction rates are consistent with the rate-determining step being the formation of a stable ion/ion orbiting complex (i.e., consistent with three-body reaction rates at the high-pressure limit). The ion/ion capture cross section is given by

$$\sigma_c = \pi[z_1 z_2 e^2/(\mu v^2)]^2 \qquad (1)$$

where v is the relative velocity of the oppositely charged ions, μ is the reduced mass of the collision partners, z_1 and z_2 are the number of units of charge on the positive and negative ions, respectively, and e is the charge on an electron. It should be noted that, given the difficulty in determining the number densities of both the anions and cations, it has not been explicitly established that the formation of a stable ion/ion orbiting complex is rate determining under the ion trap operating conditions. However, the charge-squared rate dependence has been consistently observed and this implies that the highest macroion charge states react at far higher rates than the low-charge states (e.g., a +10 ion reacts 100 times faster than a +1 ion) and the relative difference between reaction rates for ions of adjacent charge states increases as charge state decreases (e.g., a +10 ion reacts 1.23 times faster than a +9 ion whereas a +2 ion reacts 4 times faster than a +1 ion). Note also that eq 1 indicates that the cross section for ion/ion capture is inversely related to the fourth power of the relative velocity.

Several important implications for the use of ion/ion reactions to manipulate charge states can be illustrated with the simulated ion abundance versus time plots of Figure 1. This figure shows the expected evolution of positive ion charge-state abundances with mutual ion/ion storage time beginning with a selected ion of charge +14 reacting with singly charged anions present at a constant number density of 6.5 × 10^7 anions/cm^3 and a rate constant for the +1/−1 reaction of 8.2 × 10^{-8} cm^3·ion^{-1}·s^{-1}. These conditions give a +1/−1 reaction rate of roughly 5 s^{-1}, a magnitude well within the range of rates normally observed in our experiments for singly protonated proteins reacting with anions derived from perfluorocarbons. It is clear from the figure how rapidly the relatively high charge states change in abundance as a function of reaction time and how slowly the singly charged ion abundance changes. For example, the +12 ion, the abundance of which in Figure 1 reflects both the reactivities of the higher charge-state ions for its formation and the reactivity of the +12 ion for its disappearance, goes from zero abundance to its maximum abundance and to zero abundance again within roughly 20 ms of reaction time. The +1 ion, on the other hand, begins to appear as early as 50 ms after initiation of the reaction and shows

significant abundance for several hundred milliseconds beyond the 200-ms time period displayed here (data not shown). (This simulation applies to a commonly used experimental scenario in which an excess of negative ion charge, relative to the total positive ion charge, is admitted into the ion trap. The differences in the time evolution of the abundances of the various charge states is even more extreme in the case where roughly equal numbers of positive and negative charges are present. In this case, much of the charge is consumed by the highest charge states such that the number density of the oppositely charged ion decreases significantly with time.)

Figure 1 illustrates that, at any arbitrary reaction time, a range of product ion charge states is observed, with the exception of the trivial case in which all of the ions are neutralized. For example, at the time at which the doubly charged ion is most abundant, roughly equal abundances of singly and triply charged products are observed, each of which exceeds 20% of the total product ion abundance. Significant numbers of neutralized species and quadruply charged species also contribute such that relative abundance of the doubly charged ion is less that 0.5. In fact, the plot shows that none of the product ions ever exceed about 60% of the initial reactant ion abundance. Most never exceed 40% of the initial abundance. A major motivation for ion parking, therefore, is to accumulate a single charge-state ion at the expense of others and, in doing so, approach 100% of the initial multiply charged reactant abundance. Furthermore, given the combined variability in the numbers of positive and negative ions admitted into the ion trap for subsequent ion/ion reactions, the product ion charge-state distribution can vary significantly from one scan to the next, particularly for the higher charge-state product ions. This is not a particularly troublesome issue when the goal is to reduce virtually all ions to singly charged ions, where ion/ion reaction rates are already relatively low (see Figure 1). However, when the goal is to form ions of an intermediate charge state for further study, scan-to-scan variability can be problematic.

Another implication of Figure 1 for ion parking is that, for a constant diminution in ion/ion reaction rate for a selected charge state during a given ion/ion reaction period, the higher charge-state ions have a much greater probability for further reaction than the low-charge states. For example, for a 95% decrease in ion/ion reaction rate, the +1 charge-state ion of the Figure 1 simulation would decrease in rate from about 5 to 0.25 s^{-1}. Very little +1 would react at this rate over the course of a few hundred milliseconds, and effective parking of the +1 ion would result. The +12 ion, on the other hand, would go from a reaction rate of ~720 s^{-1} to a rate of 36 s^{-1}, which would lead to a significant degree of reaction to lower charge states under the condition of these simulations even with ion parking. The normal practical time frame for most ion/ion reaction periods is 10−300 ms. To minimize the extent of further reactions for a given diminution in reaction rate and for a given reaction period, it may therefore be desirable to reduce the reaction rates of highly charged ions by reducing the number of the oppositely charged reactants. As discussed further below, it is also desirable to use relatively low number densities of reactant ions to minimize space charge.

Selective Excitation of Ions on the Basis of Mass-to-Charge Ratio. The selective inhibition of ion/ion reactions relies on the exploitation of a unique characteristic of an ion that can be used to affect ion/ion reaction rates. Ion trapping instruments provide such a characteristic in that ions of each mass-to-charge ratio execute a unique set of motions at a number of characteristic frequencies.[40,43,44] The mass-to-charge-dependent frequencies of motion of ions in a pure oscillating quadrupolar field are given by

$$\omega_{n,u} = (2n \pm \beta_u)\Omega/2 \tag{2}$$

where u represents either the r-dimension (i.e., the radial plane of the ion trap) or the Z-dimension (i.e., the inter-end-cap dimension), n is an integer, Ω is the frequency of oscillation of the potential applied to the ion trap to effect ion storage, and β_u is given approximately by

$$\beta_u \cong (a_u + q_u^2/2)^{1/2} \tag{3}$$

The a_u parameter is given by

$$a_u = C_1 zeU/[m(r_o^2 + 2Z_o^2)\Omega^2] \tag{4}$$

and the q_u parameter is given by

$$q_u = C_2 zeV/[m(r_o^2 + 2Z_o^2)\Omega^2] \tag{5}$$

where the constants C_1 and C_2 depend on the specific operating mode of the ion trap,[43] U is the dc potential between the electrodes (usually = 0), V is the amplitude of the radio frequency potential used to trap the ions, r_o is the inscribed radius of the ring electrode, $2Z_o$ is the closest distance between the end-cap electrodes, and m/z is the mass-to-charge ratio of the ion. By far, the most important frequencies of motion are the fundamental secular frequencies of motion defined by the condition of $n = 0$. The application of a single-frequency waveform to the end-cap electrodes which matches the Z-dimension secular frequency of ions of a particular mass-to-charge ratio results in the Z-dimension acceleration of the ions. This is commonly done with quadrupole ion traps to eject ions within the context of the acquisition of a mass spectrum (i.e., resonance ejection[45]), to eject ions for the purpose of isolating ions of interest,[46] or to accelerate the ion so as to induce inelastic collisions with the bath gas leading to dissociation.[47] Note that eqs 2−5 apply to a pure quadrupolar field, which is impossible to achieve in a real device. Furthermore, all commercially available ion traps, as well as the ion trap used in this study, are designed to include higher-order multipole fields.[48] The existence of such fields leads to an ion frequency dependence

(43) March, R. E.; Hughes, R. J. *Quadrupole Storage Mass Spectrometry*; John Wiley & Sons: New York, 1989.

(44) March, R. E.; Londry, F. A. In *Practical Aspects of Ion Trap Mass Spectrometry, Vol. I: Fundamentals of Ion Trap Mass Spectrometry*; March, R. E., Todd, J. F. J., Eds.; CRC Press: Boca Raton, FL, 1995; Chapter 2, pp 25−48.

(45) Williams, J. D.; Cox, K. A.; Schwartz, J. C.; Cooks, R. G. In *Practical Aspects of Ion Trap Mass Spectrometry, Vol. II: Ion Trap Instrumentation*; March, R. E., Todd, J. F. J., Eds.; CRC Press: Boca Raton, FL, 1995; Chapter 1, pp 3−47.

(46) McLuckey, S. A.; Goeringer, D. E.; Glish, G. L. *J. Am. Soc. Mass Spectrom.* **1991**, *2*, 11−21.

(47) Louris, J. N.; Cooks, R. G.; Syka, J. E. P.; Kelley, P. E.; Stafford, G. C.; Todd, J. F. J. *Anal. Chem.* **1987**, *59*, 1677−1685.

(48) Stephenson, J. L., Jr.; McLuckey, S. A. *Anal. Chem.* **1997**, *69*, 3760−3766.

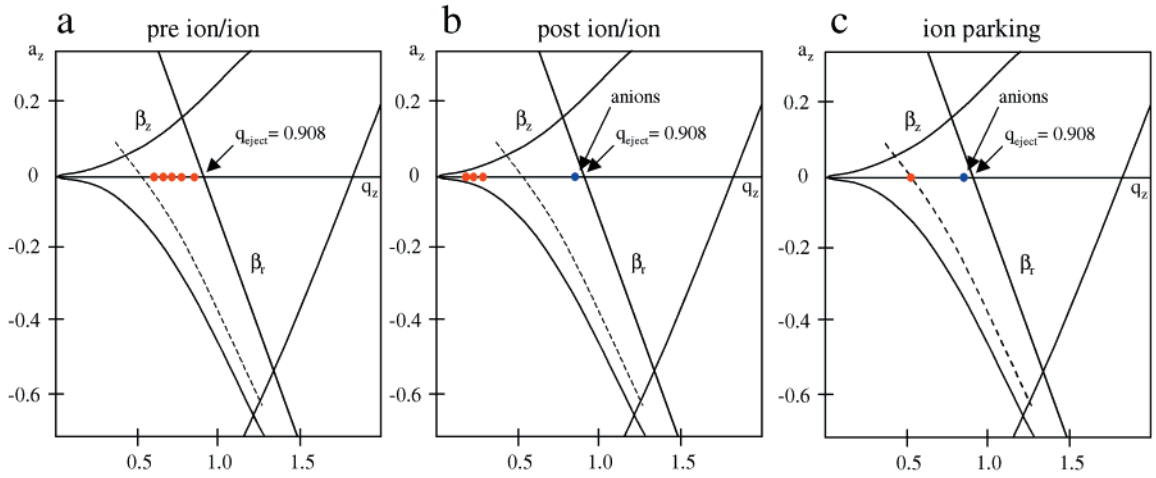

Figure 2. Schematic of the Mathieu stability diagram in (a) pre-ion/ion, (b) post-ion/ion, and (c) ion parking modes. A resonance excitation voltage of 1.0 V_{p-p} or greater at the indicated iso-β_z line is applied on either side of the ion of interest in (c).

upon ion oscillatory amplitude. This effect has important implications for ion trap mass analysis and is also expected to play a role in ion parking. However, the importance of higher-order multipole fields on ion acceleration relative to the effect of the presence of oppositely charged ion clouds, as discussed below, within the context of an ion parking experiment is not clear and is likely to be highly dependent upon the number of ions in the ion trap.

The fact that ions execute oscillatory motion with mass-to-charge-dependent frequencies of motion provides a possible means for ion parking. That is, an ion of a selected mass-to-charge ratio might be accelerated at one of its frequencies of motion while ions of opposite polarity are stored at the center of the ion trap. The rate of ion/ion reaction for the accelerated ion might be diminished relative to its rate in the absence of acceleration due either to an increase in the relative velocity of the collision pair (see eq 1), a decrease in the physical overlap of the positive and negative ions as a result of an increase in the oscillatory amplitude of the accelerated ion, or both. However, the presence of oppositely charged ion populations can have a dramatic effect on the ion acceleration behavior via the application of supplementary wave forms to the end-cap electrodes, as already demonstrated in a study of resonance ejection in the presence of oppositely charged ions.[48] It was shown that with sufficiently large numbers of oppositely charged ions resonance ejection was ineffective. Using a simple point charge picture for the relatively low mass-to-charge (singly charged) anions, it was shown that the electric field associated with the presence of the anions could exceed the effective trapping potential experienced by much higher mass-to-charge ratio positive ions resulting from the oscillating quadrupolar field. In this scenario, the positive ions could not be ejected using resonance excitation. The extent to which an ion parking experiment can be effective, therefore, is dependent upon the electric field strengths associated with the oppositely charged ion clouds.

Illustration of Ion Parking during Ion/Ion Reactions. A number of potentially useful analytical applications can be envisioned provided it is possible to selectively inhibit ion/ion reaction rates. An important example, which was alluded to above, is the ability to stop or slow a reaction at a selected product ion charge state. This would allow essentially all of the initial charge states of the ion to be accumulated into a lower charge state of the same species. Such an experiment is illustrated schematically in Figure 2 using a series of ion trap stability diagrams. The stability diagram is a plot of a_Z versus q_Z that summarizes the locations of the boundaries for stable motion in the *r*- and *Z*-dimensions. Ions are stable (i.e., they execute bounded motions) in the *r*-plane when the β_r values are between 0 and 1. Likewise, they are stable in the *Z*-dimension between β_Z values of 0 and 1. Ions are stable in both the *r*-plane and *Z*-dimension in the region of overlap between the two. The ion trap is normally operated along the $a_Z = 0$ line, such that ions of different mass-to-charge ratio fall within the stability diagram along this line with high mass-to-charge ions closest to the origin. Figure 2a illustrates an initial condition used for ion/ion reactions involving a range of multiply charged ions comprising the charge-state distribution derived from electrospray, for example, and that fall in the stability diagram at locations indicated by the red dots. The dashed line in this figure represents an iso-β_Z line, which indicates the range of *a* and *q* values that yield a constant set of *Z*-dimension frequencies. The fact that all of the red dots lie to the right of the dashed line indicates that all of the ions have *Z*-dimension secular frequencies greater than that associated with the indicated iso-β_Z line. A singly charged ion of oppositely polarity formed, for example, by glow discharge ionization, of lower mass-to-charge ratio than any of the multiply charged ions is indicated in Figure 2b by a blue dot. (The value of mass-to-charge ratio of the oppositely charged ion is important only insofar as it must be stored simultaneously with the multiply charged ions and should not fall on the iso-β_Z line used for ion parking, as discussed below.) Figure 2b shows the stability diagram after an arbitrary ion/ion reaction period in which all of the multiply charged ions have been reduced in charge such that a new and much lower charge-state distribution is formed, as represented by the shifts in position of the red dots. The blue dot does not shift, of course, as the singly charged ions are simply being consumed (neutralized) by the ion/ion reactions. Figure 2c illustrates the principle of a ion parking experiment. By applying a dipolar sine wave to the end-cap electrodes corresponding to this iso-β_Z line, any positive ions that fall at or near this point in the stability diagram (provided the electric field of the oppositely charged ions does not distort the stability diagram such that

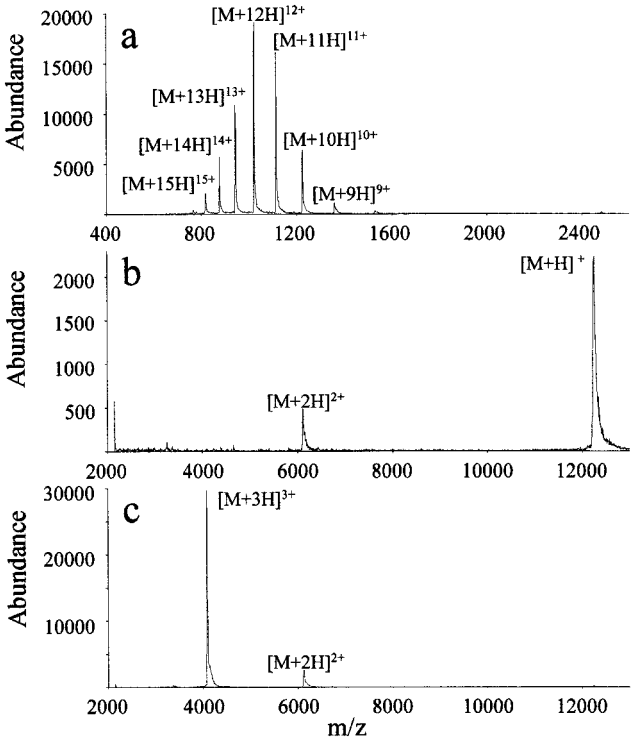

Figure 3. Mass spectra of bovine cytochrome *c* ions acquired in (a) pre-ion/ion mode, using a resonance ejection frequency of 89 202 Hz and an amplitude of 9.8 V_{p-p}, (b) post-ion/ion mode, using a resonance ejection frequency of 17 000 Hz and an amplitude of 1.5 V_{p-p}, and (c) ion parking mode, using the same resonance ejection and ion/ion conditions as described in (b), with the addition of a 1.9 V_{p-p} resonance excitation voltage at 15 000 Hz during the mutual ion storage period. The anion injection and mutual cation/anion storage periods employed in (b) and (c) were 3 and 300 ms, respectively.

resonance excitation does not occur) will be accelerated. If the ion/ion reaction kinetics of the accelerated ions is significantly reduced relative to that of unaccelerated ions of the same charge, product ions of this charge state will tend to be accumulated preferentially. In this particular example, all of the higher charge-state ions can undergo rapid ion/ion reactions until such time as they fall into the region of the stability diagram where they are "parked" by virtue of the reduced ion/ion reaction rates for the accelerated charge state.

Ions derived from electrospray of cytochrome *c* are used to demonstrate the ion parking experiment illustrated in Figure 2. Figure 3a, for example, shows the electrospray mass spectrum of bovine cytochrome *c* before anions derived from glow discharge ionization of PDCH were admitted into the ion trap (i.e., Figure 3a represents the normal electrospray mass spectrum). This spectrum represents the condition illustrated in Figure 2a. Figure 3b shows the spectrum after anions of PDCH were admitted into the ion trap for 3 ms and a mutual cation/anion storage time of 300 ms was used prior to anion ejection and subsequent mass analysis (i.e., the normal post-ion/ion reaction mass spectrum). In this case, the ion/ion reactions could proceed to the point at which the singly protonated cytochrome *c* species was the most abundant post-ion/ion reaction product cation. (Note that, based on the relative abundances of the doubly and singly charged ions in Figure 3b and the predicted abundances of Figure 1, it is likely that a significant number of the cytochrome *c* ions are completely neutralized under the conditions used to acquire Figure 3b. In fact, the extent of total neutralization is expected to be greater than that predicted on the basis of Figure 1 because the efficiency of detection of the singly charged ions is expected to be less than that of the doubly charged ions.) The spectrum of Figure 3b represents the condition illustrated in Figure 2b. Figure 3c shows the results of an experiment with ion/ion reaction conditions identical to those used to derive Figure 3b except that a single dipolar frequency of 15 kHz and 1.9 V_{p-p} was applied to the end-cap electrodes during the entire ion/ion mutual storage period. This frequency is somewhat above that of the fundamental *Z*-dimension secular frequency of the cytochrome *c* +3 charge state ion (i.e., on the low mass-to-charge side of the peak). In this experiment, it is clear that the extent of proton transfer has been significantly reduced relative to the experiment leading to Figure 3b. Furthermore, a much greater relative abundance of the +3 charge state is observed than is expected at any reaction time based on the predicted time evolution of the ion/ion reactions (Figure 1). For example, significant abundances of both the +4 and +2 ions are expected when the +3 ion is most abundant in the absence of ion parking. By accelerating ions of the mass-to-charge ratio of the +3 charge state as they are formed, the ion/ion reaction rate for this charge state is significantly diminished, thereby allowing the signal to be concentrated in this charge state. A small degree of further reaction to lower charge states is also observed and presumably occurs as a result of the finite time associated with acceleration of the newly formed +3 ion and relatively slow reactions at the elevated average velocity of the +3 ion. Ion/ion reactions can also take place during the finite length of time (several milliseconds) used to eject the anions at the end of the mutual ion storage period.

Effective ion parking experiments have been demonstrated for all charge states of cytochrome *c* from +1 to +10. Figure 4 summarizes the results for charge states +1 to +5. In all cases, significant concentration of signal in the ion for which the resonance excitation signal was most closely tuned was observed. In the case of the +1 ion, while the relative abundances in the spectra are similar in comparing Figure 3b with the relevant +1 ion parking trace of Figure 4, the absolute abundance of the ion parking experiment shows an increase of over a factor of 2. This suggests that the acceleration of the +1 ion inhibits its reaction to the neutral state.

The extent to which further reactions are observed in a ion parking experiment for a given charge state depends on the initial absolute rate of the reaction being inhibited. For example, reaction rates are highest at high charge states and with high numbers of oppositely charged ions. In this situation, the likelihood for further reactions is maximized.

A variety of ion parking experiments more sophisticated than that illustrated in Figure 3 can be envisioned. For example, sequential ion/ion reaction events with different resonance excitation frequencies in each step can allow for a sequential parking experiment whereby ions initially parked in a relatively high charge state can be moved to a second (lower) charge state in a second ion parking period. This type of procedure might be described as a sequential parking experiment. Another example is the use of multiple resonance excitation frequencies simulta-

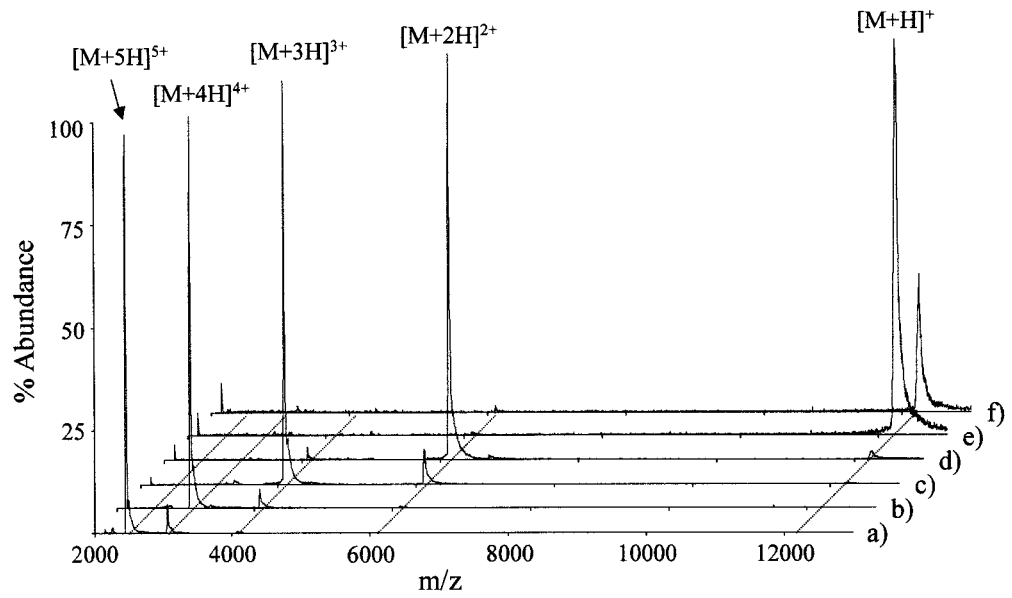

Figure 4. Post-ion/ion reaction mass spectra of bovine cytochrome *c* ions acquired in ion parking mode. Spectra were acquired using the procedure illustrated in Figure 2b. A 1.9-V_{p-p} resonance excitation voltage was applied at (a) 23 000, (b) 18 500, (c) 15 000, and (d) 10 000 Hz while for (e) a 1.2-V_{p-p} resonance excitation voltage was used at 5000 Hz. The number of anions employed in each case was varied for optimal ion parking of each charge state. The mutual ion/ion storage period was maintained at 300 ms throughout. The spectrum shown in (f) was collected under the same ion/ion reaction conditions as used in (e) in the absence of any resonance excitation voltage.

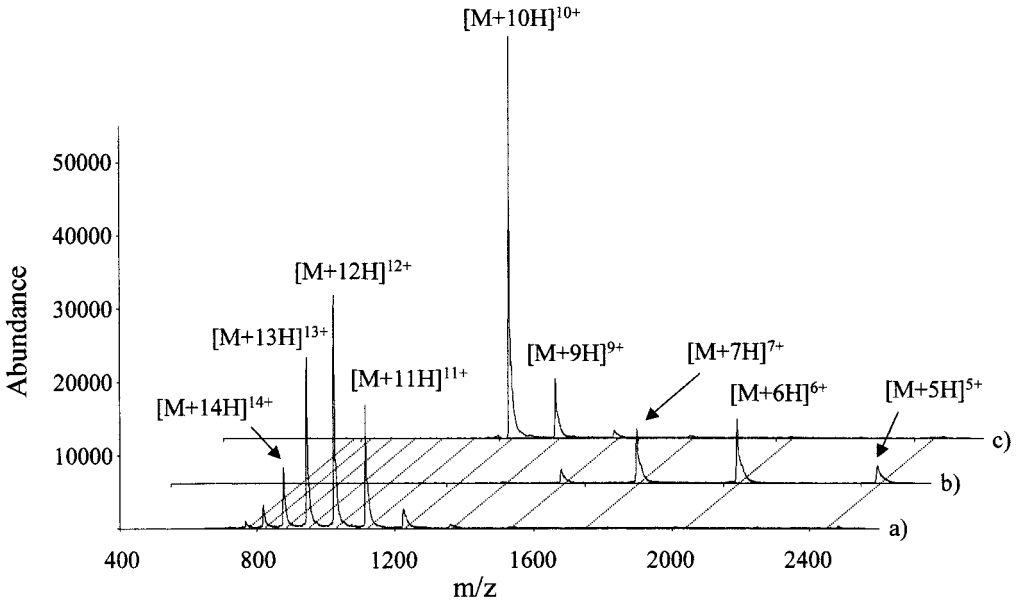

Figure 5. Mass spectra of bovine cytochrome *c* ions acquired in (a) pre-ion/ion, (b) post-ion/ion, and (c) ion parking modes (44 600 Hz, 1.25 V_{p-p}), using a resonance ejection frequency of 89 202 Hz and an amplitude of 9.8 V_{p-p}. The anion injection and mutual cation/anion storage periods used in (b) and (c) were 1 and 150 ms, respectively.

neously in a single ion/ion reaction period to allow for several ions derived from molecules of different mass to be parked simultaneously. In the case of the use of two different resonance excitation frequencies during the same ion/ion reaction period, the procedure might be referred to as a double-parking experiment.

Characteristics of Ion Parking. The experiments summarized in Figure 5 may be used to obtain a semiquantitative estimate of the efficiency of the ion parking procedure, defined as the fraction of the initial reactant ion population that can be accumulated in a specific charge state via the ion parking procedure. Figure 5a shows the pre-ion/ion electrospray mass spectrum of cytochrome *c*, Figure 5b shows the post-ion/ion mass spectrum (no ion parking) after a 1-ms anion accumulation period and a 150-ms mutual storage time period, and Figure 5c shows the results using the same ion/ion reaction conditions with a resonance excitation signal of 44 600 Hz, 1.25 V_{p-p}. This frequency corresponds to the high-frequency side of the fundamental *Z*-dimension secular frequency (in the absence of anions) of the +10 cytochrome *c* ion. An estimate of the efficiency of the ion parking experiment was made by assuming the detector response to be linear with the charge state of the ion. After normalizing ion abundances according to charge state, roughly 90% of the ions of Figure 5a are accounted for in Figure 5c. Of all of the product

ions observed in Figure 5c, roughly 83% are accounted for in the signal for the +10 ion, the remainder being accounted for by further reactions to give lower charge-state products. This comparison suggests that, under the conditions used for ion parking in these experiments, relatively few of the +10 ions are being ejected (or fragmented) such that a large fraction of the initial pre-ion/ion cation population (>70%, in this case) can be concentrated into the +10 charge state. This is an important capability because it provides a means by which analyte ions normally distributed among a range of charge states can be concentrated largely into a single charge state. As noted above, the extent of reaction beyond the charge state undergoing ion parking is related to the ion/ion reaction rate of the ion being parked. Therefore, to minimize further reaction for this relatively high charge state, a short anion accumulation time (1 ms) was used.

The resolution and efficiency of the ion parking experiment for a given charge-state ion are functions of the ion/ion reaction conditions (i.e., number of oppositely charged ions and ion storage conditions) as well as the amplitude and frequency of the resonance excitation voltage. The simultaneous presence of oppositely charged ions at the center of the ion trap can affect the resonance excitation behavior of the ions. This effect is most pronounced at high ion numbers and can have dramatic effects on mass analysis[48] and ion parking. For example, when the density of one ion polarity greatly exceeds that of the other, the application of resonance excitation to ions of the lesser density is ineffective for ion parking. This is presumably due to the electric field arising from the presence of the high-density ions. In the case of multiply charged positive ions reacting with anions derived from glow discharge ionization of PDCH, a large excess of negative charge can be effected by use of relatively long ion accumulation periods (e.g., tens of milliseconds in the present instrument configuration). However, even at anion numbers sufficiently low that resonance excitation is effective at ejecting cations, ion parking can be compromised as a result of the high ion/ion reaction rates. For these reasons, it is desirable to use the minimum anion abundance necessary for charge-state manipulation during a ion parking period. The other important ion/ion reaction condition is the level of the radio frequency voltage applied to the ring electrode used to trap ions (V in eq 5). This level is often a compromise to accommodate the wide mass-to-charge range frequently required in ion/ion reaction experiments. This level also establishes the relationship between ion frequency and ion mass-to-charge ratio (see eqs 2, 3, and 5). Of particular significance for an ion parking experiment is the fact that frequency dispersion (e.g., the difference in frequency between ions of adjacent unit mass-to-charge ratios) decreases as mass-to-charge increases and increases as the level of the radio frequency voltage increases. The use of resonance excitation during an ion/ion reaction period does not allow for an independent optimization of the level of the radio frequency voltage for ion/ion reactions and for resonance excitation.

As with any resonance excitation experiment, the effective excitation bandwidth is inversely related to the amplitude of the resonance excitation voltage. Therefore, the width of the range of mass-to-charge for which ion/ion reaction rates are affected by the resonance excitation signal, which determines the effective resolution for ion parking, is inversely related to the amplitude of the resonance excitation voltage. However, it has been observed that high ion parking efficiencies (e.g., >30%) require amplitudes of $\geq$1.0 V_{p-p} and resonance excitation frequencies of a few hundred hertz (either high or low) from the optimum frequency for resonance excitation, as judged by the point at which collision-induced dissociation efficiency is maximized in the absence of oppositely charged ions. Several factors may play roles in giving rise to this observation. First, the relative influences of the electric fields associated with the oppositely charged ions, on one hand, and the resonance excitation voltage, on the other, are expected to differ with both the number of ions and resonance excitation amplitude. Higher resonance excitation amplitudes are required when the space charge associated with the oppositely charged ions in the center of the ion trap become significant. Furthermore, the relative velocity of the ion/ion collision pair is expected to increase with resonance excitation amplitude while the spatial overlap of the oppositely charged ion clouds is expected to decrease. Therefore, relatively high resonance excitation amplitudes favor the excitation of a relatively large bandwidth of ions and also serve to minimize the ion/ion reaction rate. Good ion parking efficiencies can be observed under these conditions but at the expense of resolution.

The frequency dependence of the ion parking experiment using dipolar resonance excitation in an ion trap with a positive octopolar component (i.e., the ion trap electrode geometry of the Finnigan ion trap mass spectrometer[49,50]) is demonstrated in Figure 6. A resonance excitation amplitude of 2.3 V_{p-p} was stepped at 100-Hz increments across the +8 charge state of cytochrome *c* during an ion/ion reaction period of 300 ms (anion accumulation time, 1 ms), and selected spectra are shown here. Figure 6 shows spectra recorded at four resonance excitation frequencies applied during the ion/ion reaction period. The nominal *Z*-dimension fundamental secular frequency of the +8 charge state of cytochrome *c* under these storage conditions is 35 200 Hz, as determined from the frequency at which the maximum collision-induced dissociation efficiency was noted for the ion in the absence of anions. Figure 6 shows the results of ion parking experiments in which the resonance excitation frequencies were (a) 36 200, (b) 36 000, (c) 34 500, and (d) 34 200 Hz. Highest efficiencies are noted at 36 200 and 34 200 Hz whereas the data at 36 000 and 34 500 Hz both appear to reflect ion ejection and collision-induced dissociation associated with the resonance excitation signal. Good efficiencies could also be observed with resonance excitation amplitudes of as low as 1.0 V_{p-p} and at frequencies somewhat closer to 35 200 Hz, but much more extensive consecutive reactions to lower charge states were noted at all frequencies when lower resonance excitation amplitudes were used. Ion parking with relatively high efficiency could be effected using resonance excitation voltages at frequencies on either the high- or low-frequency sides of the fundamental *Z*-dimension secular frequency of the ion. Subtle differences in efficiency were noted in use of frequencies shifted to high- versus low-frequency sides of the parked ion, particularly at voltage levels of 2.5 V_{p-p} and higher, with the use of higher frequencies giving somewhat greater

(49) Syka, J. E. P. In *Practical Aspects of Ion Trap Mass Spectrometry, Vol. I: Fundamentals of Ion Trap Mass Spectrometry*; March, R. E., Todd, J. F. J., Eds.; CRC Press: Boca Raton, FL, 1995; Chapter 4, pp 169−202.

(50) Franzen, J.; Gabling, R.-H.; Schubert, M.; Wang, Y. In *Practical Aspects of Ion Trap Mass Spectrometry, Vol. I: Fundamentals of Ion Trap Mass Spectrometry*; March, R. E., Todd, J. F. J., Eds.; CRC Press: Boca Raton, FL, 1995; Chapter 3, pp 52−167.

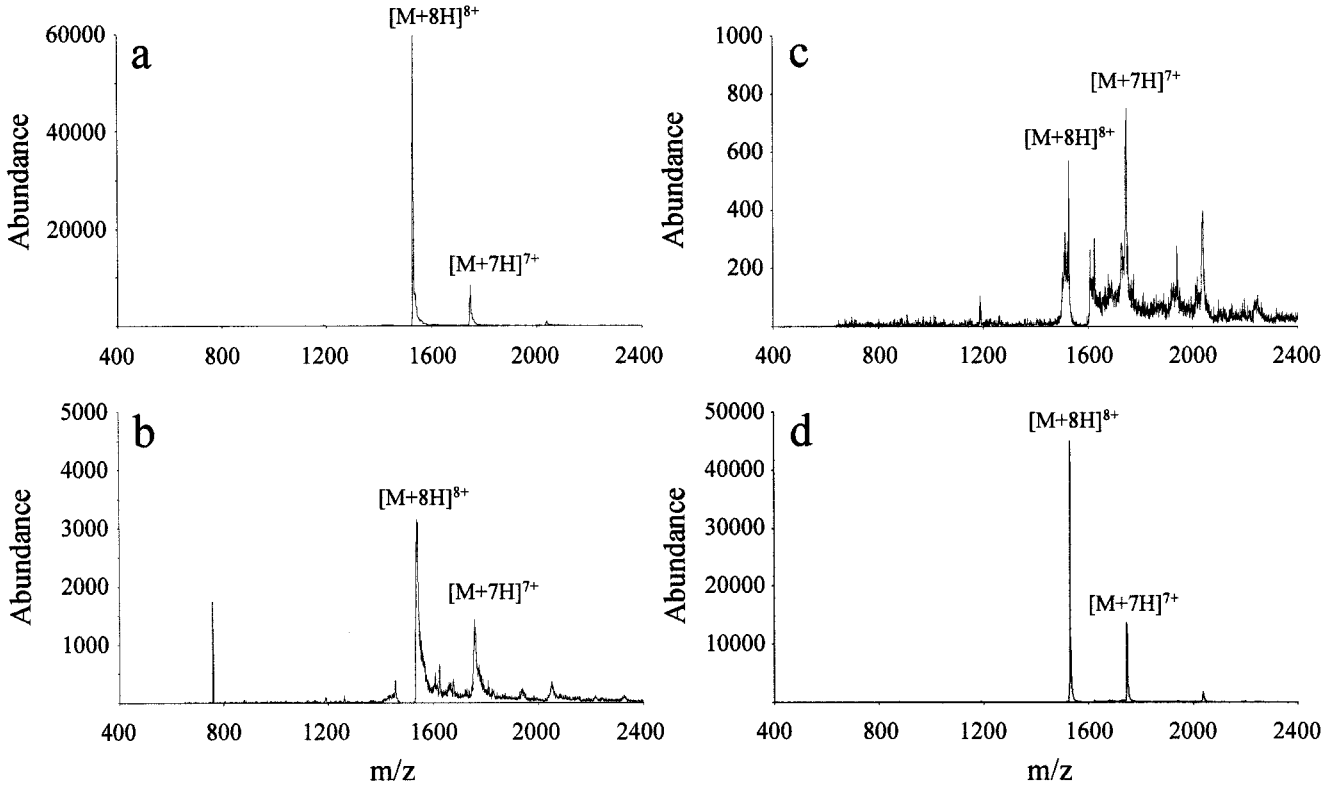

Figure 6. Frequency dependence for ion parking of the $[M + 8H]^{8+}$ ion of bovine cytochrome *c*. Spectra were acquired using a resonance ejection frequency of 89 202 Hz and an amplitude of 9.8 V_{p-p}. The anion injection and mutual cation/anion storage periods were 1 and 300 ms, respectively. A resonance excitation voltage of 1.0 V_{p-p} at (a) 36 200, (b) 36 000, (c) 34 500, and (d) 34 200 Hz was applied during the mutual ion storage period.

efficiency. This may be due to the more rapid ion acceleration associated with excitation on the high-frequency side than on the low-frequency side for ions in a nonlinear ion trap with positive octopolar character.[49,50,51] However, further detailed studies are desirable to delineate the relative merits of high- versus low-frequency resonance excitation for ion parking.

Ion Parking in a Simple Mixture Analysis Scenario. A variety of experiments involving ion parking with or without other ion manipulation techniques available with ion trapping instruments can be envisioned in dealing with the analysis of mixtures of ions derived from different compounds. The simplest involves a single ion parking resonance excitation frequency wherein only ions of a particular range of mass-to-charge ratios are accelerated to reduce ion/ion reaction rates while all other ions are allowed to react at relatively high rates. In this way, the nonparked ions can be moved to high mass-to-charge ratios (or neutralized) while the parked ions are held largely at the original mass-to-charge ratio. The spectra shown in Figure 7a−c are included to illustrate this simple experiment. Figure 7a shows the electrospray mass spectrum of an equimolar mixture of apomyoglobin and cytochrome *c*. Figure 7b shows the post-ion/ion reaction mass spectrum (no ion parking) after an anion injection period of 2 ms and an ion/ion reaction period of 50 ms. Figure 7c shows the post-ion/ion reaction mass spectrum using the same ion/ion reaction conditions as above except that a resonance excitation voltage of 1.25 V_{p-p}, 42 900 Hz was applied during the 50-ms ion/ion reaction period. This resonance excitation frequency, which is a few hundred hertz lower than that for on-resonance excitation of the +10 charge state of cytochrome *c* (*m*/*z* 1224.5), and amplitude leads to significantly greater acceleration of the +10 charge state of cytochrome *c* than any other ion associated with the mixture. It is clear from Figure 7b that, in the absence of the resonance excitation, cytochrome *c* ions shift from a charge-state range of +15 to +9 to a charge-state range of +7 to +5. Myoglobin ions shift from a charge-state range of +20 to +11 to a charge-state range of +11 to +7. (Lower charge states of myoglobin were also probably formed but fall beyond the mass-to-charge range analyzed in this experiment.) The resonance excitation voltage clearly leads to a major change in the post-ion/ion reaction mass spectrum. Much of the original cytochrome *c* ion population is concentrated in the +10 charge state. Smaller cytochrome *c* signals are observed in the +9 to +6 charge states. These signals arise from cytochrome *c* ions of initially lower charge states than +10 and reactions of ions of the +10 charge state during the resonance excitation process. The ion/ion reaction rates of the +10 ion, however, are clearly reduced relative to nonresonance excitation condition (i.e., the no ion parking experiment leading to Figure 7b). The myoglobin ions, on the other hand, appear to be much less perturbed by the resonance excitation signal. A higher myoglobin charge state distribution is observed in Figure 7c than in Figure 7b, which probably arises from off-resonance excitation of the +14 charge state and, to a lesser extent, the +13 charge state of myoglobin (*m*/*z* 1211.7 and 1304.8, respectively). Such off-resonance power absorption for these ions could lead to

(51) Williams, J. D.; Cox, K. A.; Cooks, R. G.; McLuckey, S. A.; Hart, K. J.; Goeringer, D. E. *Anal. Chem.* **1994**, *66*, 725−729.

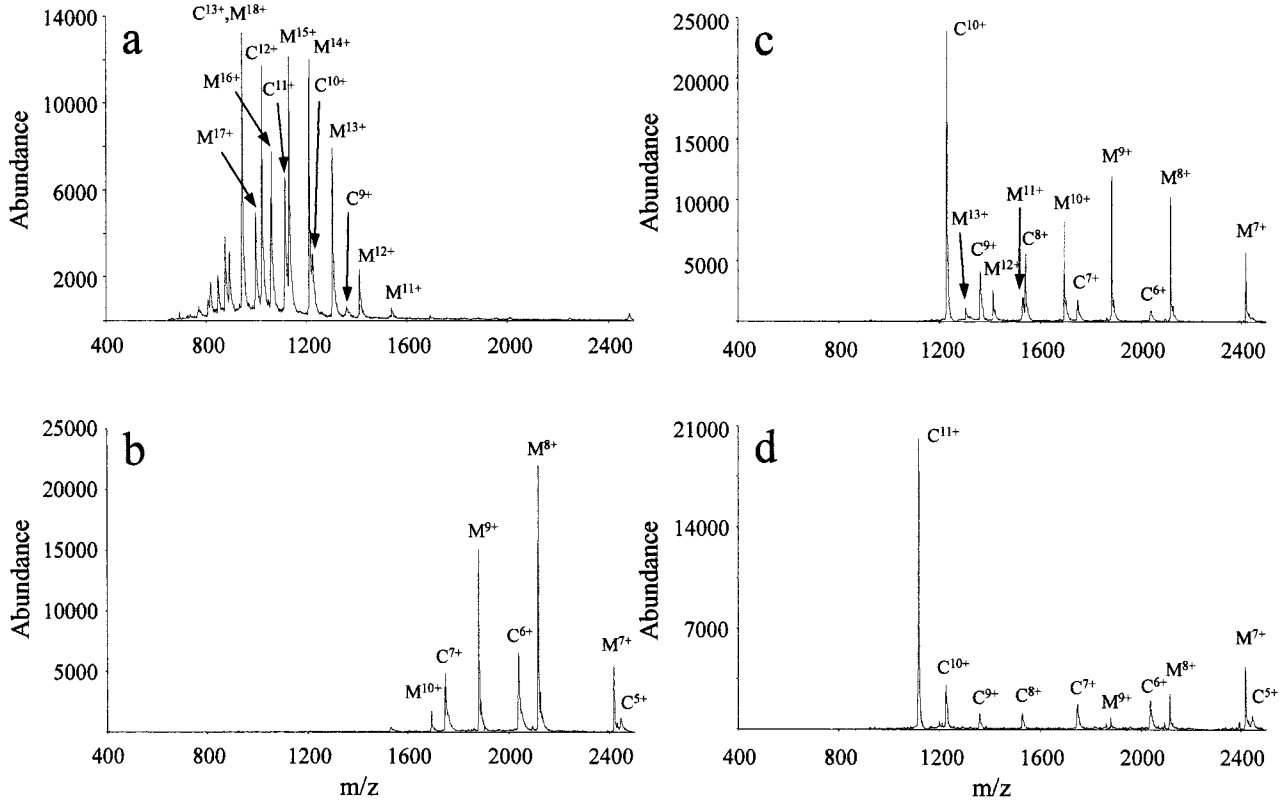

Figure 7. Electrospray mass spectra of a 5 μM bovine cytochrome *c*, 5 μM horse heart apomyoglobin solution acquired in (a) pre-ion/ion mode, (b) post-ion/ion mode, and (c) and (d) ion parking mode, using the same resonance ejection and ion/ion conditions as in (b), with the addition of a (c) 1.25-V_{p-p} resonance excitation voltage at 42 900 Hz during the mutual ion storage period, and (d) 1.25-V_{p-p} resonance excitation voltage at 47 100 Hz during the mutual ion storage period. The anion injection and mutual cation/anion storage periods employed in (b−d) were 2 and 300 ms, respectively. Mass analysis via resonance ejection at a frequency of 89 202 Hz and amplitude of 9.8 V_{p-p} was used for all spectra.

a diminution of their ion/ion reaction rates but less than that experienced by the +10 ion of cytochrome *c*.

An example of an experiment that combines more than one type of ion manipulation technique is the use of both resonance ejection, to remove ions of a particular range of mass-to-charge ratios, and resonance excitation, to park ions of a particular range of mass-to-charge ratios. This type of procedure can be effected by use of one or more resonance excitation frequencies. In the former case, however, it requires that the ions to be ejected and the ions to be parked be sufficiently spaced in mass-to-charge to allow for ejection (of one ion population) and parking (of a different ion population) to take place simultaneously. As example of such a procedure using a single resonance excitation frequency is illustrated in Figure 7d using the same mixture of myoglobin and cytochrome *c* discussed above. Figure 7d shows the spectrum acquired after an identical ion/ion reaction period as that used to acquire Figure 7b and c except that a resonance excitation frequency of 47 100 Hz and amplitude of 1.25 V_{p-p} was applied during the mutual ion storage period. This resonance excitation signal leads to ejection of the +16 charge state of myoglobin and parking of the +11 charge state of cytochrome *c*. This single resonance excitation frequency serves simultaneously to eject all myoglobin ions of charge states +16 and higher, since the highest charge states of myoglobin must fall into the +16 charge state before proceeding to lower charge states, and inhibits the ion/ion reaction rate of the +11 cytochrome *c* ions. The +10 charge-state ions of cytochrome *c* are likely to arise from the fraction of +11 cytochrome *c* that undergoes an additional ion/ion reaction and possibly from a small degree of parking arising from off-resonance power absorption from the applied resonance excitation voltage. The cytochrome *c* and myoglobin ions observed at lower charge states arise primarily from the original +10 and lower charge states of cytochrome *c* and the +15 and lower charge states of myoglobin. These ions are not subjected to either resonance ejection or parking and can therefore react with the stored anions. Lower charge states are observed in Figure 7d than in Figure 7b because less positive charge is available for reaction to consume negative charge in the combined ion ejection/ion parking experiment. When there are comparable numbers of positive and negative charges, the extent of charge-state reduction of the multiply charged ions is sensitive to both the numbers of anions and numbers of cations.

The data of Figure 7d illustrate one approach to the removal of ions from one protein while retaining ions of the other protein. This example also shows that the point at which ion parking is carried out can be within the charge-state envelope of the pre-ion/ion reaction charge-state distribution. The example of Figure 3, on the other hand, provided a case in which ion parking was used at a point well below the lowest charge state observed in the pre-ion/ion reaction condition. One can envision a wide variety of other uses of ion parking in conjunction with more or less conventional ion isolation procedures applied before, during, or after the ion parking experiment. The optimal strategy is expected to be determined largely by the mixture analysis scenario.

CONCLUSIONS

It is possible to affect (i.e., diminish) selectively the rates of ion/ion reactions in a quadrupole ion trap via the acceleration of ions at mass-to-charge-dependent frequencies of motion. The approach is only effective when the electric field associated with the presence of the oppositely charged ion clouds is sufficiently small that it does not seriously affect the resonance excitation process. The condition in which ions of a selected mass-to-charge window are accelerated so as to reduce the ion/ion reaction rate is termed "ion parking". The efficiency of the process can be high with an efficiency of >70% demonstrated here. A variety of applications of this technique can be envisioned to be analytically useful. One involves the accumulation of a large majority of ions initially formed with a distribution of charge states into a single charge state. This is an attractive capability when, for example, it is desirable to acquire tandem mass spectrometry data. Another set of applications pertains to mixture analysis whereby the ion parking capability adds a new tool to the ion trap suite of ion isolation techniques.

ACKNOWLEDGMENT

Research supported by the National Institutes of Health under Grant GM 45372 and the Purdue Research Foundation.

Received for review August 31, 2001. Accepted October 23, 2001.

AC0109671